

COMPARING CO₂ STORAGE AND ADVECTION CONDITIONS AT NIGHT AT DIFFERENT CARBOEUROFLUX SITES

M. AUBINET*, P. BERBIGIER¹, CH. BERNHOFER², A. CESCATTI³,
C. FEIGENWINTER⁴, A. GRANIER⁵, TH. GRÜNWARD²,
K. HAVRANKOVA⁶, B. HEINESCH, B. LONGDOZ⁵, B. MARCOLLA³,
L. MONTAGNANI⁷** and P. SEDLAK⁸

Unité de Physique des Biosystèmes, Faculté Universitaire des Sciences agronomiques de Gembloux, 8, avenue de la Faculté, B-5030 GEMBLoux, Belgium; ¹INRA, Ephyse, Villenave d'Ornon, France; ²Technical University of Dresden, Germany; ³Centro di Ecologia Alpina, Trento, Italy; ⁴Institute of Meteorology, Climatology and Remote sensing, University of Basel, Switzerland; ⁵INRA, Ecologie et Ecophysiologie forestière, Nancy, France;

⁶Institute of Landscape Ecology, Academy of Sciences of the Czech Republic (ASCR) Brno, Czech Republic; ⁷DISAFRI, University of Viterbo, Italy; ⁸Institute of Atmospheric Physics AS CR, Praha, Czech Republic

(Received in final form 6 November 2004)

Abstract. Anemometer and CO₂ concentration data from temporary campaigns performed at six CARBOEUROFLUX forest sites were used to estimate the importance of non-turbulent fluxes in nighttime conditions. While storage was observed to be significant only during periods of both low turbulence and low advection, the advective fluxes strongly influence the nocturnal CO₂ balance, with the exception of almost flat and highly homogeneous sites. On the basis of the main factors determining the onset of advective fluxes, the ‘advection velocity’, which takes net radiation and local topography into account, was introduced as a criterion to characterise the conditions of storage enrichment/depletion. Comparative analyses of the six sites showed several common features of the advective fluxes but also some substantial differences. In particular, all sites where advection occurs show the onset of a boundary layer characterised by a downslope flow, negative vertical velocities and negative vertical CO₂ concentration gradients during nighttime. As a consequence, vertical advection was observed to be positive at all sites, which corresponds to a removal of CO₂ from the ecosystem. The main differences between sites are the distance from the ridge, which influences the boundary-layer depth, and the sign of the mean horizontal CO₂ concentration gradients, which is probably determined by the source/sink distribution. As a consequence, both positive and negative horizontal advective fluxes (corresponding respectively to CO₂ removal from the ecosystem and to CO₂ supply to the ecosystem) were observed. Conclusive results on the importance of non-turbulent components in the mass balance require, however, further experimental investigations at sites with different topographies, slopes, different land covers, which would allow a more comprehensive analysis of the processes underlying the occurrence of advective fluxes. The quantification of these processes would help to better quantify nocturnal CO₂ exchange rates.

Keywords: Advection, CO₂ storage, Forest ecosystems.

* E-mail: aubinet.m@fsagx.ac.be

** Present affiliation: Autonomous Province of Bolzano, Agency for the Environment, Italy.

1. Introduction

There is increasing evidence that the rise of atmospheric carbon dioxide concentration (hereafter $[\text{CO}_2]$) resulting from anthropogenic CO_2 emissions is the main cause of climate warming. The role of the terrestrial biosphere and, in particular, of forests in mitigating or delaying such an effect is of the utmost importance, since the biosphere absorbs about one third of human-induced CO_2 emissions (Schimel, 1995; Watson et al., 2000).

The net ecosystem exchange (NEE) of CO_2 between forests and atmosphere is the result of the difference between two large fluxes: plant photosynthesis and respiration. NEE can be directly quantified at different time scales (daily, seasonal, annual) through micrometeorological measurements using the eddy covariance (EC) technique. This technique is based on the high-frequency measurement of the vertical wind speed and of the $[\text{CO}_2]$ above plant canopies (turbulent eddy flux), coupled with measurements of CO_2 storage below the measurement point using slow response infrared gas analysers (Aubinet et al., 2000). First implemented in 1951 (Swinbank, 1951), the EC technique has been used more and more frequently in the last decade and is now applied at more than 200 sites (Baldocchi, 2003). Further to providing an assessment of NEE, the method is unrivalled when it comes to describing and studying ecosystem response to climate. The integration of NEE data collected over forest ecosystems with other spatial information (meteorology, land cover, phenology) has already enabled a first estimation of carbon sequestration by European forests (Papale and Valentini, 2003).

In spite of its success, however, the EC technique does have shortcomings. In particular, during stable conditions at night (light winds), an underestimation of the CO_2 fluxes using the EC method frequently occurs (Goulden et al., 1996; Jarvis et al., 1997; Aubinet et al., 2000, 2002). This is because non-turbulent transport processes, not taken into account by the EC system, become significant under these conditions. The main processes taking place under these conditions are the storage of CO_2 in the air space below the measurement height and consequent drainage by advection. The importance of advection at night has been given more emphasis recently (Lee, 1998; Baldocchi et al., 2000; Pawu et al., 2000; Aubinet et al., 2003; Staebler and Fitzjarrald, 2004; Feigenwinter et al., 2004; Marcolla et al., in press). As the night flux error acts as a selective systematic error (Moncrieff et al., 1996), its impact on the net CO_2 exchange and on the estimation of the carbon sequestration by the forest is quantitatively important. A small nighttime bias error of $1 \mu\text{mol m}^{-2} \text{s}^{-1}$, aggregated for 12-h nights over one year, is equivalent to $189 \text{ g C m}^{-2} \text{ year}^{-1}$. Errors of this magnitude can produce unrealistic annual sums that cannot be supported by independent biological measurements of tree and plant growth.

Currently, an empirical correction is applied to compensate for the underestimation of nighttime flux measurements (Fan et al., 1995; Goulden et al., 1996; Falge et al., 2001; Gu et al., 2004). This correction is based on CO₂ flux measurements obtained during windy periods and on the friction velocity (u_*) that allows one to differentiate between a windy period and a non-turbulent period (light winds). This correction remains, however, difficult to apply as it depends on the relative importance of storage and advection at the site (Aubinet et al., 2002).

In order to produce defensible measurements of net annual carbon fluxes, it is necessary to better understand the processes at work during stable conditions in forest ecosystems and, in particular, the conditions under which storage and advection occur in relation to climate, site topography and land cover.

Our aim is to compare the conditions in which CO₂ storage and advection take place at different sites in order to characterise their relative importance in relation to site topography, land cover and meteorological conditions.

2. Theory

2.1. CO₂ BUDGET EQUATION

The carbon dioxide mass conservation equation states that the CO₂ produced or absorbed by the biological source/sink is either stored in the air or removed by flux divergence in all directions. This equation has been developed and discussed in detail, notably by Finnigan (1999), Finnigan et al. (2003) and Feigenwinter et al. (2004). After applying Reynolds decomposition, spatial integration over a control volume of height h , ignoring the horizontal turbulent flux divergence and the horizontal variation of the vertical flux, and applying the continuity equation, the equation is reduced to:

$$\begin{aligned} \text{NEE} = & \int_0^h \frac{1}{V_m} \left[\frac{\partial \bar{c}}{\partial t} \right] dz + \frac{1}{V_m} (\overline{w'c'})_h + \int_0^h \frac{1}{V_m} \bar{w}(z) \frac{\partial \bar{c}}{\partial z} dz \\ & + \int_0^h \frac{1}{V_m} \left(\bar{u}(z) \frac{\partial \bar{c}}{\partial x} + \bar{v}(z) \frac{\partial \bar{c}}{\partial y} \right) dz, \end{aligned} \quad (1)$$

where NEE represents the biological source/sink strength term, c is the CO₂ mixing ratio, V_m is the molar volume of dry air, u , v and w represent the instantaneous velocity components in the horizontal (x , y) and vertical (z) directions, respectively, overbars represent time averages and primes departures therefrom. The four terms on the right-hand side represent, respectively, the storage of CO₂ in the air of the control volume, the vertical turbulent transport, the vertical advection and the horizontal advection. In

most of the experiments, the sites are assumed to be sufficiently homogeneous for the NEE estimations be based on the turbulent transport and the CO₂ storage measurements, the two advection terms being neglected. As this hypothesis seems generally reasonable during daytime, it is more questionable in nocturnal conditions.

Lee (1998) was the first to propose an estimation of the vertical advection term (V_h) as:

$$V_v = \frac{1}{V_m} \bar{w}_h (\bar{c}_h - \langle c \rangle), \quad (2)$$

where w is the vertical component of the velocity measured at the control volume top depurated of topography and sensor misalignment effects, \bar{c}_h is the [CO₂] at the control volume top and the vertically averaged [CO₂], $\langle c \rangle$, is defined as:

$$\langle c \rangle = \frac{1}{h} \int_0^h \bar{c}(z) dz. \quad (3)$$

This expression was used in several studies (Lee, 1998; Baldocchi et al., 2000; Paw et al., 2000) to derive estimates of NEE that take account of the vertical advection. However, this approach is still incomplete as it neglects the horizontal advection. This point was notably raised by Finnigan (1999) who argued that horizontal advection could possibly be of the same order of magnitude as the vertical advection. Later, budget equations using the Lee approach for the vertical advection, and taking into account the horizontal advection term, were used by Aubinet et al. (2003), Staebler and Fitzjarrald (2004) and Feigenwinter et al. (2004). A general definition of horizontal advection is:

$$V_h = \int_0^h \frac{1}{V_m} \left(\bar{u}(z) \frac{\partial \bar{c}}{\partial x} + \bar{v}(z) \frac{\partial \bar{c}}{\partial y} \right) dz. \quad (4)$$

However, at single sloping sites during stable periods, as the flow is driven mainly by buoyancy, the air movement can be considered as mainly two-dimensional so that (4) reduces to:

$$V_h = \int_0^h \frac{1}{V_m} \bar{u}(z) \frac{\partial \bar{c}}{\partial x} dz. \quad (5)$$

2.2. EXPERIMENTAL REQUIREMENTS

The assessment of the advection terms based on Equations (2), (3) and (4) or (5) is a challenging task. It requires notably the measurement of the vertical

velocity (Equation (2)) and of the horizontal [CO₂] gradient (Equations (4) and (5)), which are very small and often close to the resolution limit of the apparatus. The vertical velocity measurements can be contaminated by the horizontal velocity. The angles used to rotate the velocity in order to deduce its vertical component should thus be accurately computed and take into account the tilt due to the surface slope and the deflection by the sonic or the supporting structure. The method followed to perform these rotations is described below.

The horizontal [CO₂] gradient measurement requires a carefully designed sampling system that avoids calibration mismatches, systematic and positioning errors. Calibration mismatches can be avoided by using the same infrared gas analyser (IRGA) to measure the [CO₂] in the same horizontal transect or by performing a continuous intercalibration when several analysers are used. Systematic errors may appear due to a pressure difference in the IRGA chamber. In order to avoid them, the sampling system should be devised so that all points are measured under the same chamber pressure. Vertical positioning of the sampling points is also critical, since the vertical [CO₂] gradient is much greater than the horizontal gradient. A small error in the sampling height can lead to a contamination of the horizontal gradient by the vertical one.

Sampling frequency should also be taken as large as possible in order to take account of short term [CO₂] variations. In view of the limited number of measurements than can be made by a single IRGA during one measurement period (typically, one half-hour), a compromise should be obtained in order to optimise the number of IRGAs that are used, the number of samples per period and the number of sampling points.

3. Materials and Methods

3.1. SITE DESCRIPTION

Experiments were developed independently at six sites: Bily Kriz (Czech Republic), Hesse (France), Le Bray (France), Renon (Italy), Tharandt (Germany) and Vielsalm (Belgium). All these sites were part of the European Union funded CARBOEUROFLUX network, which aims at investigating carbon and energy exchanges of terrestrial ecosystems in Europe. More details about this network are given in Valentini (2003). The site characteristics that are most pertinent for the present study are given in Table I, as well as references where more information about the sites can be found.

3.2. MATERIAL

All the sites under investigation were equipped with the standard CARBOEUROFLUX eddy covariance system, and we applied the standard

TABLE I
Site characteristics.

	Le Bray	Vielsalm	Renon	Tharandt	Hesse	Bily Kriz
Region	Les Landes	Ardennes	Italian Alps	Ore mountains	Lorraine	Beskydy mountains
Latitude	44°42' N	50°18' N	46°35' N	50°58' N	48°40' N	49°30' N
Longitude	0°46' E	6°00' E	11°26' E	13°34' E	7°05' E	18°32' E
Elevation(m)	60	480	1730	380	300	800–900
Topography	Flat	Single slope	Single slope	Hilly	Single slope	Single slope
Average	<0.2%	3%	10%	4%	3%	25%
Slope	–	South–east North–west	North–west South–east	North–east South–west	South–east North–west	North–north–east South–south–west
Main species	Pinus pinaster Ait	Fagus sylvatica, L.Pseudotsuga mensiensii [Mirb.] Franco.	Picea abies [L] Karst	Picea abies [L] Karst	Fagus sylvatica, L.	Picea abies [L] Karst
Tree age (years)	34	98–68	Unevenly aged	108	36	25
Tree density (stems ha ⁻¹)	500	45–49	270	477	3800	2500
Tree height (m)	18	27–36	31	27	12.7	9.5
LAI	2.6–3.1	5.0		8	7.8	9.0
Understorey	0–1.5	none		Sparse	Sparse	None
References	Berbigier et al. (2001).	Laitat et al. (1999).	Montagnani (1999), Cescatti and Marcolla (2004)	Grünwald (2002)	Granier et al. (2000a, 2000b)	Havrankova and Sedlak (2004)

methodology described by Aubinet et al. (2000). The EC systems were used to measure the vertical turbulent fluxes of momentum, sensible heat, water vapour and carbon dioxide. They were also used to give an estimate of the boundary-layer stability (via the Obukhov length) and of the vertical component of the velocity at the tower top.

In addition to this set-up, systems devised to measure [CO₂] and wind velocities at several locations were installed for temporary campaigns at each site. Their characteristics are given in Table II. Although the set-ups differed from site to site, all the systems had common features: one to three vertical profiles of [CO₂] and wind velocity were measured. Wind velocities were measured using sonic anemometers and [CO₂] using infrared gas analysers. Vertical profiles of [CO₂] included 4 to 13 points, according to the sites. In each case, a system involving pumps, tubes, filters and vanes was devised to carry the sampled air to the IRGA. Even if different compromises were chosen at the different sites, each system was designed in order to minimise the calibration, systematic and positioning error mentioned in Section 2.2. At the sites where horizontal [CO₂] gradients were measured, a single IRGA was used in order to avoid calibration mismatches. Systematic measurement errors due to a pressure difference in the chamber were avoided by using tubes of the same lengths for each sampling point and/or by using a two-pump system, one to transport the air at a high flow rate from the sampling point to a reservoir maintained at the atmospheric pressure, and the other to sub-sample the air at a lower rate from the reservoir to the IRGA. Positioning errors were minimised by carefully choosing the height of the sampling points in order to avoid any contamination by the vertical gradient. In addition, at Vielsalm and Hesse, the horizontal [CO₂] gradient was measured along a transect composed of six sampling points in order to check the gradient reproducibility. Sampling frequency was taken higher than at least nine sampling per half hour at each site but one. Half-hourly averages of the measured variables were used in the analyses.

Additional information about site devices is given in Aubinet et al. (2001, 2003) for Vielsalm and Hesse, Feigenwinter et al. (2004) for Tharandt, and Marcolla et al. (in press) for Renon.

3.3. METHODS: ESTIMATION OF THE FLUXES

3.3.1. *Storage*

The storage is defined as:

$$S_c = \int_0^z \frac{\partial \bar{c}}{\partial t} dz. \quad (6)$$

TABLE II
System characteristics.

	Le Bray	Vielsalm	Renon	Tharandt	Hesse	Bily Kriz
<i>Campaign dates</i>	July–December, 2002	A. June–September, 2002 B. May–June, 2003	A. June–August, 2000 B. June–August, 2002	September–October, 2001	July–November, 2003	A. May–October 2002 B. June–August 2003
<i>Anemometer profiles</i>						
Type	A & B. Gill R2 + UPB sonics	A & B. Gill R2/R3	A & B. Gill R2/R3	Gill R2, CSAT3, Gill HS	Gill R3 + UPB sonics	A. Cup An. B. Therm. + Cup An.
Number of vertical profiles (number of point by profile)	A. 3 (5 + 2 + 2) B. 1 (5)	A. 1 (5) B. 1 (2)	A. 1 (5) B. 1 (2)	3 (3 + 2 + 2)	1 (3)	A. 1 (6) B. 1 (10)
Measurement heights [m]	A. 3, 6, 3, 10, 14, 22, 40 B. 3, 10, 14, 22, 40	A. 1.3, 13.3, 22.4, 31.6, 41 B. 4, 32	A. 1.3, 13.3, 22.4, 31.6, 41 B. 4, 32	2.5, 0.5 id. + 42	3, 6, 22	A. 5, 6, 7, 9, 13, 15 B. 0.25, 0.5, 1, 1.75, 5, 6, 7, 9, 13, 15
<i>Concentration measurements</i>						
Analyser type	A & B. LI-6262 LI-800	A & B. LI-6262	B. LI-6262	4 LI-6262	LI-6262	LI-800

TABLE II
Continued

	Le Bray	Vielsalm	Renon	Tharandt	Hesse	Bily Kriz
Number of vertical profiles (number of points by vertical profile)	1 (13)	A & B. 3 (8 + 4 + 4) aligned	B. 3 (6 + 4 + 4) aligned	3 (12 + 8 + 8) in triangle	3 (6 + 4 + 4) aligned	A. 1 (6) B. 3 (2) aligned
Measurement heights [m]	0.06, 0.4, 1.6, 2.8, 4.8, 8, 15.4, 17, 19, 23, 30, 35, 41	A & B. 0.5, 1, 3, 6 id. + 16, 24, 32, 36	B. 1, 2, 4, 8 Id. + 16, 32	0.1, 0.3, 0.5, 1, 2, 2.5, 8, 26 id. + 33, 37, 40, 42	0.5, 1, 3, 6 0.2, 0.7, 2, 5, 2, 10, 4, 22	A. 0.5, 1, 2, 3, 7, 12 B. 0.4, 0.75
Maximum horizontal distance between vertical profiles [m]	-	A & B. 89	B. 100	40-50	83	B. 75
Number of sampling points of the horizontal transect	-	A & B. 6	B. 3	3 (triangle)	6	B. 3
Number of samplings during one half hour	-	A & B. 9	B. 1	15	9	

It is deduced from the half-hourly variation of $[\text{CO}_2]$ sampled at different heights according to:

$$S_c = \frac{1}{\tau} \sum_{i=1}^n \Delta \bar{c}_i h_i, \quad (7)$$

where τ is the duration of the time interval (1/2 h), the summation index corresponds to the different sampling points and h_i is a weighing height characterising each $[\text{CO}_2]$ measurement level.

3.3.2. *Advection*

Vertical advection computation is made by using Equations (2) and (3). Its estimation thus requires at least one vertical profile of $[\text{CO}_2]$ and one measurement of the vertical velocity at the top of the control volume when the linearity assumption of the vertical velocity profile is introduced. At most of the sites, the vertical component of wind velocity was obtained from high frequency three-dimensional (3D) anemometric measurements applying a correction to the raw velocity according to the planar fit method (Wilczak et al., 2001). This method allows the prediction of the expected vertical velocity due to topography and sensor misalignment for wind coming from a given direction. A rotation angle in the u–w plane (β) is estimated from long-term observations of the wind vector, which is assumed to be a function of the wind direction only (azimuthal angle α). It is therefore estimated by fitting a sinusoidal regression on the $\beta(\alpha)$ graph and assuming that $\bar{\beta}$ (and thus \bar{w}) was zero over a long period for all wind directions. In order to reduce the spread of β estimations, only periods of near-neutral stratification were selected for this estimation (Finnigan, 1999).

Horizontal advection estimations are based on Equation (4) or (5). They require simultaneous measurements of the vertical profiles of wind velocity and of horizontal $[\text{CO}_2]$ gradients. At Hesse, Renon, Vielsalm and Bily Kriz, where the slope can be considered as uniform, the flow was supposedly two dimensional and the horizontal $[\text{CO}_2]$ gradient was deduced from a single transect. At Tharandt, which is characterised by a more complex topography, a three-dimensional approach was followed and the horizontal gradients were deduced from three vertical profiles placed at the vertexes of a triangle. The instrumental set-up and the procedure for data analysis are described in detail by Feigenwinter et al. (2004).

In view of the preceding sign conventions, a positive (negative) advection corresponds to a CO_2 removal from (supply to) the control volume.

4. Results and Discussion

4.1. STORAGE

The averaged daily course of the CO₂ storage is given in Figure 1 for each site. Even if the storage flux does not have the same importance at each site, it evolves in a similar way: positive storage is observed at night and negative storage in the morning. The first situation corresponds to a CO₂ build-up in the canopy that takes place under stable conditions, and the second to the release of this CO₂, following either turbulence or leaf assimilation onset. The importance of the storage flux varies by about a factor of 10 from site to site: the averaged storage flux calculated between 1600 and 0400 was larger than $2 \mu\text{mol m}^{-2} \text{s}^{-1}$ at Le Bray, about $1 \mu\text{mol m}^{-2} \text{s}^{-1}$ at Vielsalm and Tharandt, $0.4 \mu\text{mol m}^{-2} \text{s}^{-1}$ at Hesse, and $0.2 \mu\text{mol m}^{-2} \text{s}^{-1}$ at Renon and Bily Kriz. Such variability can be explained partly by differences in source intensity (different soil organic matter quantity and quality, and different temperatures) and canopy height (storage volume), but it is also due to differences between advection and turbulence regimes.

Another notable feature in Figure 1 is represented by the low CO₂ storage values during the second part of the night – three times smaller than during the first part of the night. This is remarkable because it was observed at sites characterised by very different topographies, vegetation cover and wind regimes. The reason for this fall is not clear, but the mass conservation equation suggests that it should be due to either a decrease in source intensity or an increase in the CO₂ transport processes.

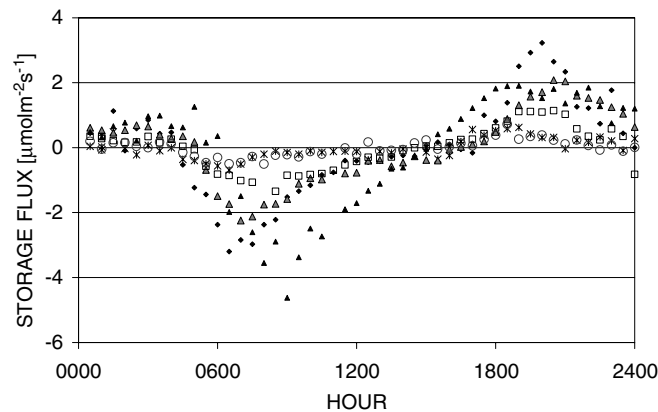


Figure 1. Diurnal course of the storage flux at four sites. Only observations from June to August have been selected for the graph: Vielsalm and Hesse: 1997 to 2002, Tharandt: 2001, Renon, Le Bray and Bily Kriz : 2002. Legend: Open circles: Bily Kriz, Black squares: Hesse, Black triangles: Le Bray, Open squares : Renon, Open triangles: Tharandt, Black diamonds: Vielsalm.

A decrease in source intensity may result from soil cooling (as the temperature is the main driving variable of respiration), or from decreased CO_2 diffusion due to saturation in CO_2 of the air close to the soil surface. None of these processes, however, explains such an important reduction. Soil respiration measurements made using an automatic chamber at the Vielsalm site (Perrin et al., 2004) showed that the relative decrease of respiration during summer nights was lower than 20%, which is far smaller than the reduction observed. Also, the hypothesis concerning the gradient decrease does not appear to be realistic in view of the very high $[\text{CO}_2]$ observed in the soil (several thousands of $\mu\text{mol mol}^{-1}$ compared to several hundreds of $\mu\text{mol mol}^{-1}$ in the air (Pumpannen et al., 2003).

The most likely explanation of the decrease in storage is therefore an increase in the transport processes. However, no increase in turbulent transport can be invoked here as the average friction velocity did not differ significantly between the first and second parts of the night. In addition, the storage response to turbulence was clearly different between the two parts of the night: at Vielsalm, in particular, values of the storage flux for identical u_* were two to three times greater during the first part of the night compared to the second part (Figure 2).

The remaining explanation would thus be an increase in advection as a non-turbulent transport process. However, the advection estimations presented below are not precise enough to support this hypothesis. Accuracy of these measurements should still be improved and analysis of other terms in the CO_2 balance (horizontal turbulent flux divergence, in particular) should be developed in order to better understand this behaviour.

We now compare the response of storage to turbulence and advection at each site. In order to eliminate any effect of the respiratory source intensity,

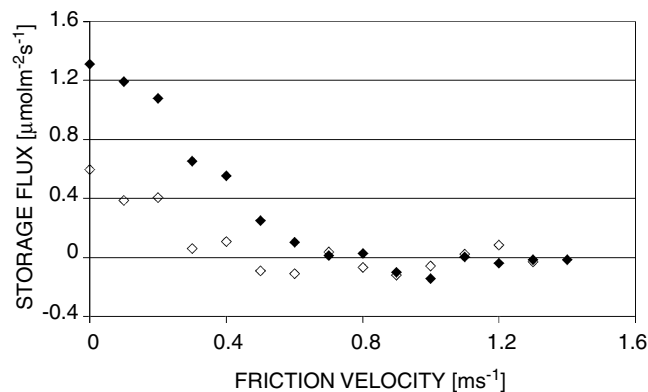


Figure 2. Evolution of the storage flux vs the friction velocity at Vielsalm in nocturnal conditions. Closed points: before midnight, Open points: after midnight. Data selection: all conditions, 1997 to 2002 (39,081 points).

the storage was normalised with the CO₂ source intensity, due to ecosystem respiration. It was parameterised by an exponential function of the temperature (Lloyd and Taylor, 1994, Equation (11)):

$$F_{\text{cn}} = R_{10} \exp \left\{ 308.56 \left(\frac{1}{56.02} - \frac{1}{(T - 227.13)} \right) \right\}, \quad (8)$$

in which the respiration at 10 °C (R_{10}) was estimated for each site on the basis of soil respiration chamber measurements. Consequently, the normalised storage can be interpreted as the proportion of the respired CO₂ stored in the air below the measurement system.

The evolution of the normalised storage flux with friction velocity for the six investigated sites is given in Figure 3a; the average night values were calculated between 1800 and 0400 and grouped according to increasing u_* . It is clear that, at all sites, the storage was insignificant at high friction velocities. This is logical as storage takes place only in the absence of other transport processes, particularly in the absence of turbulent transport. At very low friction velocities, however, very contrasting situations occur. At the Le Bray site, which is flat and relatively homogeneous, the normalised flux reached about 0.8, suggesting that 80% of the CO₂ produced by the respiration at night is stored in the air below the measurement point. The evolution of the turbulent flux with u_* (data not shown) suggests that the remaining 20% was removed by turbulence. At Tharandt, Vielsalm and Hesse, which are gently sloping sites (2–4%) and at Renon and Bily Kriz, situated on steeper slopes (about 20%), the normalised storage did not exceed 0.4 and 0.1, respectively. The part of the CO₂ removed from the ecosystem therefore reached 60% and more than 90%, respectively. As this corresponds to small u_* values, the CO₂ removal cannot be explained by turbulence. This suggests that, except at Le Bray, non-turbulent transport such as advection takes place at the sites.

In order to confirm this, we look at the dependence of storage on advection. To do this, we introduce an index similar to the free convective velocity scale as introduced by Tennekes and Lumley (1972) and Jacobs et al. (1994). We call this the ‘advection velocity’ (u_{adv}), defined as:

$$u_{\text{adv}} = \left(- \left(\frac{R_{\text{net}}}{\rho C} \right) \left(\frac{g}{T} \right) h \sin \theta \right)^{1/3}, \quad (9)$$

where R_{net} is the net radiation, ρC is the thermal capacity of the air, T is the absolute temperature, g is the gravity acceleration, h is a scaling length and θ is the slope angle. In the following results, h was fixed at 10 m. This index may be related to the average velocity established along slopes under the action of buoyancy and surface drag and thus to the mass flow generated by

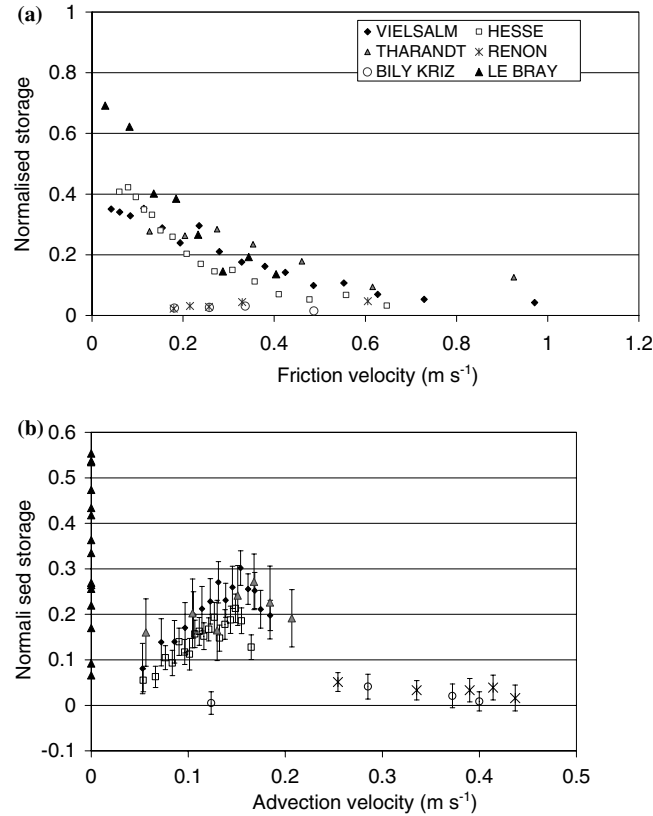


Figure 3. Evolution of the normalised storage flux according to friction velocity (a) and advection velocity (b). Night averaged values were computed between 1800 and 0400 and classed by increasing u_* (a) or u_{adv} (b). Selected periods: Vielsalm and Hesse: January 1997 to December 2002, Tharandt: January to December 2001, Renon: June to August 2002, Bily Kriz: July to October 2002, Le Bray: July to December 2002. One point corresponds to averages on 10 nights (220 measurements) for Renon and Bily Kriz, 30 nights (660 measurements) for Le Bray, 50 nights (1100 measurements) for Tharandt, 100 nights (2200 measurements) for Hesse and Vielsalm. Legend same as Figure 1.

katabatic winds. This index is therefore expected to measure the importance of advection fluxes generated along the slopes by gravity flows. Justifications about the expression for this velocity are given in Appendix I.

The evolution of normalised storage according to advection velocity is presented for all sites in Figure 3b, which shows that the storage is low at high advection velocities. This is especially clear over steep slopes, as at Renon and Bily Kriz, but also over more gentle slopes (Vielsalm, Hesse, Tharandt) where a decrease of storage with u_{adv} was observed above 0.07 m s^{-1} . Here again, these results are logical since storage can take place only in the absence of transport processes and, particularly in this case, in the

absence of advection. At the two first sites, the advection is due to katabatic flows generated by buoyancy along the slope. Due to the steepness of the slope, these flows are generated almost every night, which explains the very low storage values. On more gentle slopes these flows also develop, but to a lesser extent. They become significant only under strong negative net radiation, which is characterised by u_{adv} values above 0.07 m s^{-1} . The largest storage values were observed at the Le Bray site, where the slope is zero and no katabatic winds occur. These high values suggest that the occurrence of a high advection is rare at this site.

At u_{adv} values lower than 0.07 m s^{-1} , the index probably becomes less relevant. Indeed, in this range, low u_{adv} values correspond generally to low net radiation and are often associated with turbulent periods. Therefore, the increase in storage that was observed below 0.07 m s^{-1} probably reflects, indirectly, a response of storage to turbulence that is not characteristic of the advection processes.

We may conclude from this analysis that, used together, the friction and the advection velocities allow the appearance of storage to be determined: it becomes significant when both the turbulent and the advective transports are limited. This corresponds to u_* and u_{adv} lower than 0.4 m s^{-1} and 0.07 m s^{-1} , respectively.

This analysis could be refined, as follows. First, the u_{adv} index could be improved by taking into account the differences in surface roughness that may induce strong differences between sites. Also, the analysis only considers advection flows stemming from gravity flows and does not take into account possible breezes resulting from land-use heterogeneities.

4.2. HORIZONTAL ADVECTION

Horizontal advection estimation requires a knowledge of vertical profiles of horizontal velocity and concentration gradients.

4.2.1. *Horizontal Velocities*

In nocturnal conditions, horizontal velocities can be induced at the local level by vegetation cover heterogeneity, drainage flows or mesoscale circulations. The resulting flow patterns are generally 3D and the measurement of horizontal advection therefore requires a complex measurement system with at least three sampling profiles (Feigenwinter et al., 2004). On single slopes, however, horizontal wind velocities are due mainly to gravity flows generated by buoyancy. In these conditions, they are aligned parallel to the steepest slope direction. This makes the analysis simpler as the flow pattern can be considered as 2D. This is the case, in particular, at Renon, Vielsalm, Hesse and Bily Kriz. For the first three sites, the presence of gravity flows under

nocturnal conditions is confirmed by the wind rose, as shown in Figure 4. Indeed, the nocturnal wind roses differ from those measured during the day as they always show a peak corresponding to the steepest slope direction. This is north in Renon (Figure 4b) and south-east in Hesse and Vielsalm (Figures 4d and f). In contrast, during diurnal conditions, no clear preferential direction appears (Figures 4a, c, e) excepted for Renon, which is characterised by a typical breeze circulation regime and where a preferential wind direction (south-south-west) is also observed during daytime (Figure 4a).

The average nocturnal velocity profiles at Renon, Vielsalm and Bily Kriz are presented in Figure 5; all velocities are normalised by their value at the

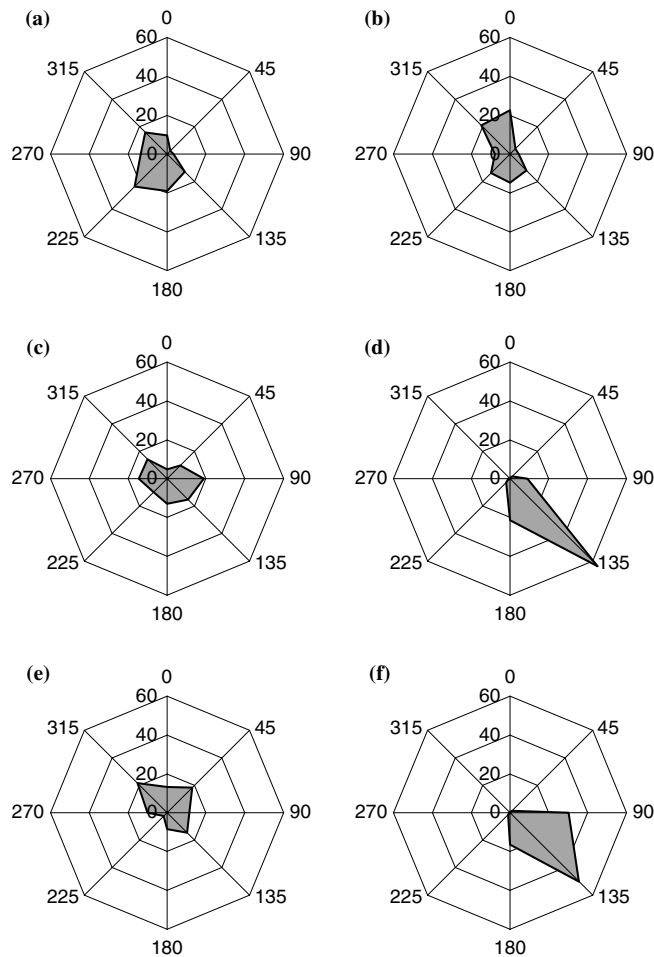


Figure 4. Wind roses of horizontal velocities under diurnal and nocturnal conditions. a, c, e (b, d, f): day (night) conditions at Renon, Vielsalm and Hesse, respectively. The velocity measurement heights are respectively 32, 3 and 3 m.

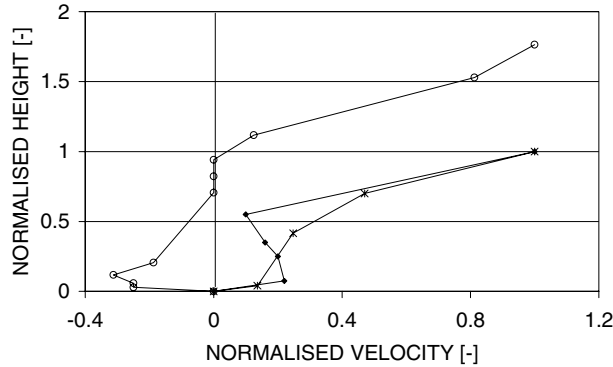


Figure 5. Vertical profiles of horizontal velocity during stable conditions at Renon, Vielsalm and Bily Kriz. Velocities are normalised by their value at the tower top. Legend: same as Figure 1.

tower top. In all cases the velocities close to the soil are all oriented downslope; the negative value observed at Bily Kriz results from the fact that the velocity at the tower top is upslope. The Renon profile is monotonic, in contrast with those of Vielsalm and Bily Kriz that present secondary maxima. This suggests that above- and below-canopy flows are coupled in Renon and decoupled in Vielsalm and Bily Kriz. At the two latter sites, the gravity flow is confined below the canopy, while at Renon it develops within the whole canopy height. As a result, the velocity measured at the tower top characterises the katabatic flow, which is confirmed by the pattern of the corresponding wind rose (Figure 4b).

The degree of coupling between above- and below-canopy flows depends on the depth of the boundary layer in which the katabatic flow develops (katabatic boundary layer, KBL) and on the leaf area density (LAD) distribution in the canopy. Notably, the depth of the KBL depends on the distance from the hill crest. Models describing the evolution of the velocity field in KBL flows were developed by Manins and Sawford (1979) and Kondo and Sato (1988). The latter predicted that the KBL depth (i.e., the height at which the minimum velocity is reached) would increase with distance from the crest at a rate depending mainly on the bulk heat exchange coefficient, and thus on momentum and heat roughness lengths (z_o and z_T , respectively). They predicted that for a “rough” terrain (i.e. $z_o = 0.32$ m, $z_T = 0.01$ m), at 100, 500 and 3000 m from the crest (which corresponds approximately to the positions of measurement points at Bily Kriz, Vielsalm and Renon), the boundary-layer depth would reach 7, 12 and 45 m, respectively, corresponding with the observations above.

The profile differences between the sites could also be explained by differences in LAD distributions, as these determine both the distribution of momentum (drag) sinks in the canopy and the thermal stratification. Indeed,

under nocturnal conditions, the leaves act as heat sinks due to radiative cooling. LAD patterns are given in Figure 6a for Renon, Bily Kriz and Vielsalm; the leaves are concentrated mainly in the lower half of the canopy (below 12 m high) at Renon and in the upper half of the canopy (between 20 and 40 m) at Vielsalm. At Bily Kriz, even if the maximum LAD was observed in the lower canopy part, the cumulated leaf area in the upper quarter of the canopy is comparable to those of Vielsalm, due to a higher leaf area index (LAI). The temperature profiles reflect well these contrasting situations (Figure 6b), the largest gradients being observed close to the soil at Renon, which is more typical of an open canopy, and close to the canopy top at Vielsalm and Bily Kriz, which are characterised by closed canopies. The strong temperature inversion that appears at the canopy level at the latter two sites would form an obstacle to any perturbation emanating from above. It is thus an additional cause of decoupling between above- and below-canopy flows.

4.2.2 $[CO_2]$ Horizontal Gradient

Horizontal $[CO_2]$ gradients measured at 1-m height in nocturnal conditions are given in Figure 7 for Hesse, Renon and Vielsalm; this shows that either positive (i.e., in the same direction as the wind velocity) or negative (i.e., opposite to the wind velocity) gradients may be observed under advection conditions. The data presented in Figure 7 are averaged over long periods and denote systematic behaviours.

The average horizontal gradients at Hesse and Vielsalm were $+0.025 \mu\text{mol mol}^{-1} \text{m}^{-1}$ and $-0.028 \mu\text{mol mol}^{-1} \text{m}^{-1}$, respectively; the $[CO_2]$ was found to evolve regularly from point to point, confirming the longitudinal repeatability of the measurements. At Vielsalm, a second transect displaced laterally by 50 m from the first one was measured; a similar gradient (dotted line) was found, confirming the representativity of the measurements. At Renon, a

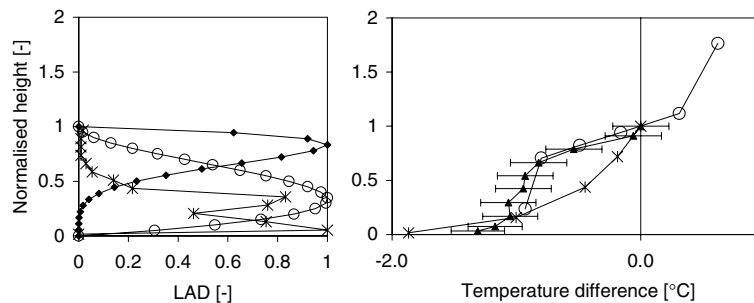


Figure 6. (a). Leaf area density distribution at Renon, Vielsalm and Bily Kriz. (b). Vertical temperature profiles at Renon, Vielsalm and Bily Kriz during night conditions. Legend: same as Figure 1.

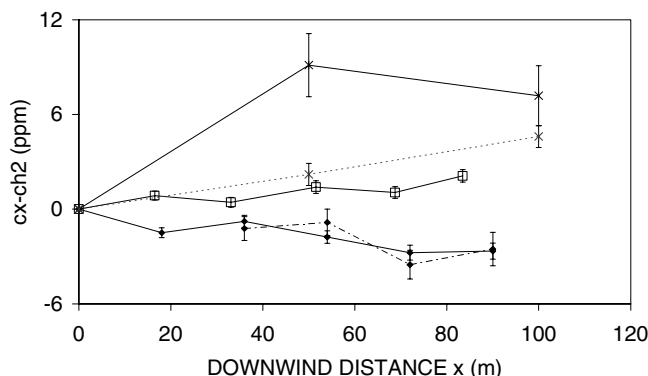


Figure 7. Horizontal profiles of CO₂ measured in the slope direction in nocturnal conditions at Vielsalm, Hesse and Renon. Solid line for Renon: 1 m high. Dotted line for Renon: 8 m height. Solid line for Vielsalm: beech transect. Dotted line for Vielsalm: Douglas fir transect. Legend: same as Figure 1.

larger gradient was observed at 1-m height but appeared to be subject to a higher variability: about $+0.18 \mu\text{mol mol}^{-1} \text{m}^{-1}$ in the first transect part, $-0.039 \mu\text{mol mol}^{-1} \text{m}^{-1}$ in the second part and $+0.079 \mu\text{mol mol}^{-1} \text{m}^{-1}$ on average. This is probably because the central point is in a forest gap colonised by grass where the [CO₂] is generally higher at nighttime. This shows the high sensitivity of the horizontal gradient to source term heterogeneities.

Both positive and negative horizontal [CO₂] gradients are theoretically conceivable. On one hand, the air passing through a control volume can be enriched in CO₂ thanks to the respiration of the sources situated in the volume. On the other hand, in the presence of vertical entrainment, it is mixed with air arising from above the canopy that is poorer in CO₂ and can thus be depleted in CO₂. Both processes compete and can lead to either situation. In order to better understand the conditions of the appearance of positive or negative horizontal gradients, a simple model that describes the evolution of the [CO₂] in a KBL was developed. This considers the KBL as a single layer that flows along the slope and is fed by air entrained vertically at its top (entrainment hypothesis, Manins and Sawford, 1988; Aubinet et al., 2003). The air is poorer in CO₂ above the KBL, compared to within, so that the entrainment induces a dilution of the CO₂ of the KBL. On the other hand, the soil respiration is simulated by a source placed at the soil level that produces CO₂ at a constant rate. In order to reach an analytical solution of the problem, the entrained mass flow and source intensity were presumed to be constant all along the slope, although this is not essential for the qualitative analysis that is made here. In addition, similarity of the vertical profiles of horizontal velocity and tracer concentration gradients was assumed, no particular hypothesis being made about the profile shapes. The soil

respiratory rate, the entrainment rate and $[\text{CO}_2]$ at the KBL top constituted the boundary conditions and the initial horizontal mass flow and the vertical tracer concentration gradient, the initial conditions. More details about the model are given in Appendix II.

The model showed first that, in the absence of entrainment, the horizontal gradient can only be positive, the source term always enriching the KBL in CO_2 . In the presence of entrainment, the model showed that, at a long distance from source heterogeneities, the $[\text{CO}_2]$ tends towards a uniform equilibrium value and the horizontal $[\text{CO}_2]$ gradient disappears. Consequently, in conditions of uniform entrainment, horizontal gradients appear only downslope of any CO_2 source intensity heterogeneities. They are positive if the sources situated upslope are stronger than at the measurement point and negative in the converse situation. The distance necessary for the equilibrium to recover after a change in source intensity depends on the horizontal and vertical mass fluxes; our estimates suggest that this could reach several hundreds of metres, indicating that horizontal heterogeneous conditions may be the rule rather than the exception in forests.

In conclusion, the model described above confirms that, in the presence of entrainment, either positive or negative gradients could be observed at the sites, depending on the CO_2 source repartition upslope from the measurement transect. This hypothesis is still to be tested, and would require extensive measurements of the respiratory sources in the areas surrounding the measurement points. Besides, this analysis should be refined to take into account the possible lateral exchanges that could occur at sites where there is no privileged direction.

4.2.3. *Advection Estimations*

The sign of the horizontal gradient determines the sign of the advection terms. The results given in Figure 7 clearly show that horizontal advection is positive at Renon and Hesse (CO_2 is removed from the control volume) and negative at Vielsalm (CO_2 is brought to the control volume). A negative horizontal advection was also observed at Tharandt in more complex conditions (Feigenwinter et al., 2004). The model predicted that both positive and negative advection are possible. In the absence of air entrainment, positive advection should take place. In the presence of entrainment and heterogeneity of source intensity, either positive or negative horizontal advection may appear, depending on the source/sink distribution. In the absence of new heterogeneities, however, the KBL tends to an equilibrium after a few hundred metres, and horizontal advection should disappear. Under these conditions, in the absence of storage or turbulence, the source term is thus compensated only by vertical advection. This is the situation that

was described by Lee (1998) and that would be reached in conditions of horizontal homogeneity.

The computation of advection fluxes also requires knowledge of the profile shape of the horizontal [CO₂] gradients. Marcolla et al. (in press), has suggested that these gradients decay at about 16 m at Renon; at Vielsalm this height is even smaller, about 6 m. These results suggest that the transport of CO₂ by horizontal advection does not take place in the whole KBL but only in its lower part, in agreement with Staebler and Fitzjarrald (2004). As a result, the horizontal advection order of magnitude varies from 0.5 to 5 μmol m⁻² s⁻¹ at Renon (Marcolla, et al., in press) and from 0.1 to 1 μmol m⁻² s⁻¹ at Vielsalm. More experimental studies and modelling efforts are needed to better understand the CO₂ distribution in the KBL and to better describe the vertical profiles of horizontal [CO₂] gradients and improve horizontal advection estimates.

4.3. VERTICAL ADVECTION

The vertical advection can be estimated from Equations (2) and (3). It therefore requires an estimation of the vertical velocity and the vertical profiles of [CO₂].

4.3.1. Vertical Velocities

The evolution with stability of vertical velocities measured at the tower top is presented in Figure 8. The results show that, even if no clear tendency was observed under unstable conditions, the velocities during stable conditions are often negative, i.e., directed to the soil. This was the case at all the sites, except Hesse where the vertical velocity remained close to zero across the whole stability range. At Bily Kriz, significantly negative values were

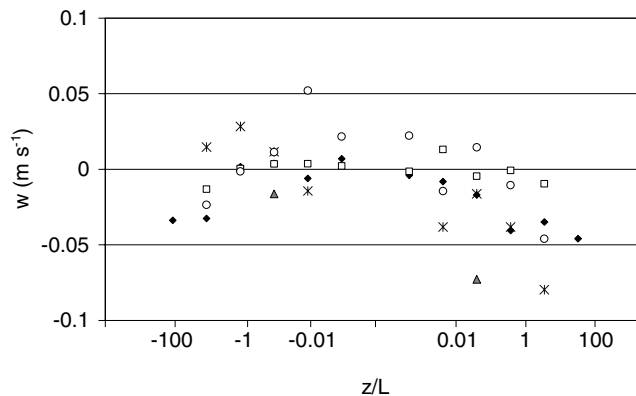


Figure 8. Evolution of vertical velocity (w) with stability at five sites. Legend: same as Figure 1.

observed only under very stable conditions. Negative velocities characterised a vertical flow towards to the soil. In the cases of sloping sites, Aubinet et al. (2003) suggested that the negative velocities were due to entrainment of the air above the canopy by the katabatic flow, but could also be an effect of natural convection, due to leaf cooling.

Values of the average vertical velocities varied greatly from site to site: they were about 0.02 m s^{-1} at Vielsalm but reached 0.07 m s^{-1} in Tharandt and Renon. The origin of these differences is not clear. However, the measurements should be interpreted differently at each site, as they correspond to different conditions. It was shown in Section 4.2 that the point where the vertical velocity was measured was located in the KBL at Renon and situated well above at Vielsalm and Bily Kriz. In these latter sites the vertical velocity could not be representative of the real entrainment, and vertical profiles of vertical velocity would be necessary to better quantify the entrainment.

Let us also remark that the vertical velocity observations at the sites are coherent with the horizontal $[\text{CO}_2]$ gradient observations and the KBL model predictions. Indeed, at Hesse, where the vertical velocity was close to zero, the gradient was positive while at Tharandt and Vielsalm, where negative gradients were observed, measurements clearly indicated a negative vertical velocity. This is in agreement with the model, which predicted that in the absence of entrainment, the horizontal $[\text{CO}_2]$ gradient should be positive, and that a negative vertical velocity was a necessary condition to observing a negative horizontal $[\text{CO}_2]$ gradient.

4.3.2. $[\text{CO}_2]$ Vertical Gradient

Vertical profiles of $[\text{CO}_2]$ are presented for nocturnal and diurnal conditions in Figures 9a and b; in each case, the height is normalised by the canopy height. Vertical profiles of the difference between daytime and nighttime $[\text{CO}_2]$ are also presented in Figure 9c. All the $[\text{CO}_2]$ vertical gradients exhibited the typical daytime and nighttime patterns: they were all negative and larger in absolute value close to the soil. In addition, the average concentrations were systematically higher at night than during the day. The night CO_2 accumulation was the greatest at Le Bray and greater at Vielsalm and Hesse than at Renon and Bily Kriz (Figure 9c), confirming the results presented in Figure 3. Under diurnal conditions, the gradients were also negative at all sites, except at Renon and Le Bray where they were zero. This can be explained by the more open character of the canopy at these sites compared to the others, as already shown by the temperature profile (Figure 6) for Renon.

4.3.3. Advection Estimates

In view of the $[\text{CO}_2]$ gradient and vertical velocity signs, the vertical advection will always be positive when significant (i.e., at four of the sites studied

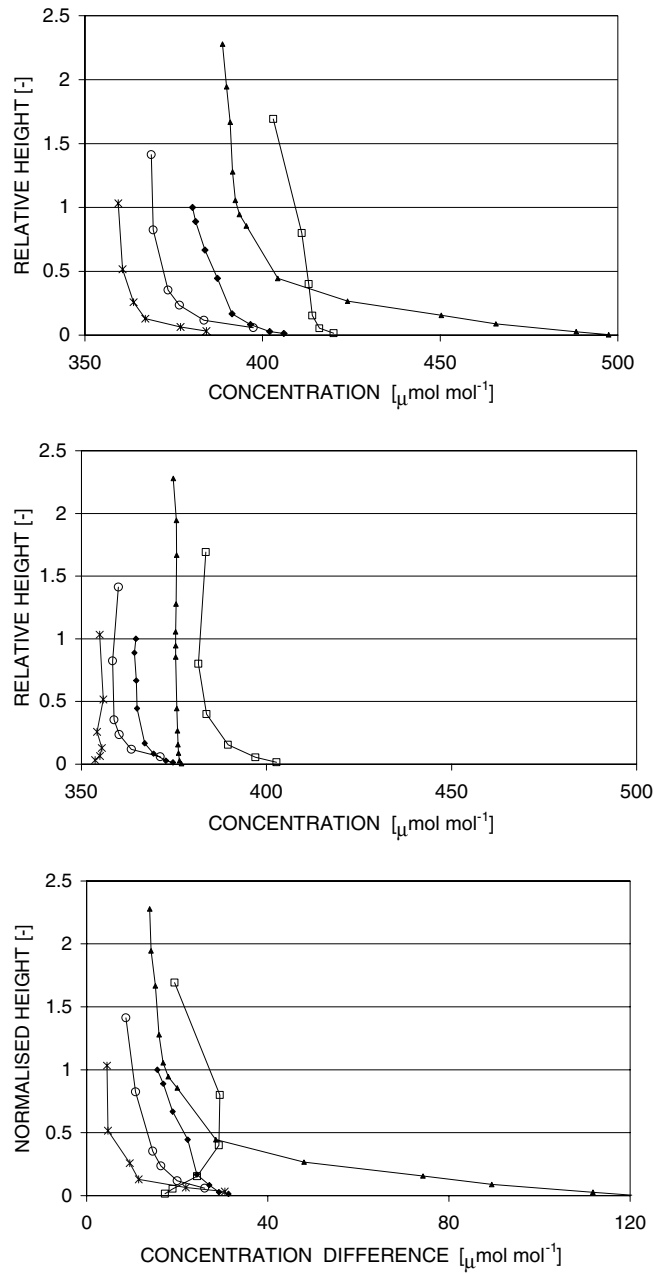


Figure 9. Vertical profiles of CO₂ concentration at Bily Kriz, Le Bray, Hesse, Renon and Vielsalm. (a) nocturnal conditions, (b) diurnal conditions, (c) differences between night and day. Legend: same as Figure 1.

here). Vertical advection will thus always contribute to remove CO₂ from the control volume. On the basis of the [CO₂] profiles and vertical velocities presented here, the order of magnitude of vertical advection varied from 0.1 μmol m⁻² s⁻¹ at Bily Kriz to more than 5 μmol m⁻² s⁻¹ at Renon and 10 μmol m⁻² s⁻¹ at Vielsalm. These values are simple averages, however, and do not take into account the large variability of these fluxes, depending notably on the stability. As no estimation of the vertical velocity was made at Le Bray, it was not possible to evaluate vertical advection at this site. In addition, the high advection values at Vielsalm resulted from high estimations of vertical velocity. This variable was thought not to be representative of the real entrainment process and could be overestimated.

5. Conclusions

Nighttime CO₂ transport processes were investigated at six CARBOEUROFLUX sites. During periods of low turbulence, storage and advection were found to be the main processes at work in the canopy. The relative importance of storage and advection varied greatly from site to site, being mainly determined by the local slope. At the flat site of Le Bray, advection was negligible and most of the CO₂ produced by respiration was stored in the air below the measurement point. In contrast, at steeply sloping sites (Renon, Bily Kriz), the CO₂ storage was almost insignificant and the advection was the main transport process. At moderately sloping sites (Tharandt, Hesse, Vielsalm), the two processes coexisted and their relative importance varied depending on the weather conditions: advection was important, especially under low turbulence and strong negative net radiation; storage was significant in the absence of both turbulence and advection. A criterion (u_{adv}) based on net radiation and site topography was introduced in order to select the periods when storage became important.

The advection fluxes were globally positive (i.e., corresponding to a removal of CO₂ from the ecosystem) but were distributed differently between vertical and horizontal advection: at one site (Hesse), vertical advection was almost zero and horizontal advection positive; at three other sites, vertical advection was positive, with positive horizontal advection at one site (Renon) and negative horizontal advection at two others (Vielsalm, Tharandt). This shows that the nighttime CO₂ balance can present very different patterns from site to site, depending on the topography (slope, distance from the hill ridge), land cover (LAD distribution, surface roughness) and horizontal source heterogeneities.

The computation of the CO₂ advection fluxes and the description of the conditions in which they appear remain difficult and require further experi-

mental and theoretical research. In particular, further investigation is needed, as follows:

- The decrease in storage after midnight that was observed at all sites remains unexplained. It was shown that it could not be ascribed to a source decrease or to a turbulence onset. It is thus presumed to be due to an increase of advection in the second part of the night. This would make sense as advection takes place on sloping sites under the action of buoyancy, following surface cooling, and thus appears more likely in the second part of the night. At present, advection measurements are not accurate enough to allow this hypothesis to be checked. In addition, this hypothesis is challenged by the Le Bray results where the storage decrease was also observed while no advection was found at this site.
- The u_{adv} criterion was useful for distinguishing sites dominated by storage and by advection. The validity of the criterion needs to be confirmed by more measurements at more sites with different topographies. In addition, the criterion could be refined by introducing roughness parameters for which roughness measurements at the sites should be performed.
- Either positive or negative horizontal [CO₂] gradients were observed at each site. We built a model that predicted these signs to be linked to entrainment and to the direction of the heterogeneity. These predictions need to be verified. Extensive measurements are required to describe the source repartition at the sites more accurately.
- Knowledge of the vertical distribution of the horizontal [CO₂] gradient is necessary to allow an accurate estimation of the horizontal advection flux. This gradient has been measured only at a few sites. More measurements of the vertical distribution of the horizontal gradient are needed at the sites, as well as a theoretical investigation that predicts the evolution of the [CO₂] field in the KBL.
- The measurement of vertical velocity is essential to the determination of vertical advection. First, the position of the measurement appears critical. It should be made at the top of, or within, the KBL in order to represent the real entrainment exerted by the KBL on the ambient air. In sites where the KBL is confined below the canopy, this would require placing an additional sonic anemometer in or below the canopy. In addition to the measurement position, the method is very sensitive to measurement uncertainties. Aubinet et al. (2003) estimated a 1° error in tilt angle to induce 0.025 to 0.06 m s⁻¹ errors in vertical velocity and 2.5 μmol m⁻² s⁻¹ on the flux. Alternative and more robust methods of estimating w could be investigated. One possibility would be to deduce w from the mass conservation equation by using several vertical profiles of horizontal velocities. In single sloping sites, a minimum of two profiles would be enough if

- lateral flows were ignored. In spite of technical difficulties, this method would have the advantage of integrating the measurement on the whole transect and being more representative than a single point estimation of w .
- Finally, the analysis presented here focused on advection generated by gravity flows along single slopes. It did not address the problem of more complex topographies that could generate 3D movements, or of breezes that could be generated by land cover heterogeneities and might even affect flat sites.

Acknowledgements

This research was supported by the European Commission, Programme Environment and Climate, project CARBOEUROFLUX under contract EVK2-CT-1999-00032. In addition, the Belgian team was supported by the Fonds National de la Recherche Scientifique (Belgium), the Italian team by the Forest Department of the Autonomous Province of Bolzano (Italy) and the Foundation Cassa di Risparmio di Trento e Rovereto (Italy). The authors would like to thank all the people that help them to conceive, build and maintain the experiments: Jean Marc Bonnefond and Didier Garrigou at Le Bray, Patrick Gross at Hesse, Michel Yernaux at Vielsalm and Hesse, Dr. Barbara Köstner, Dr. Roland Vogt, Uwe Eichelmann, Heiko Prasse, Horst Hebentanz, and Andreas Christen at Tharandt, Günther Kerschbaumer at Renon, Dalibor Janous and Marian Pavelka at Bily Kriz.

Appendix I

Consider a parcel of air submitted to surface drag and buoyancy. The surface drag τ is expressed by (Arya, 1988):

$$\tau = \rho C_M u^2, \quad (\text{A1})$$

where C_M is the drag coefficient, ρ the air density and u the velocity of the parcel.

The buoyancy per unit area, F_B , is expressed by (Kondo and Sato, 1988):

$$F_B = \rho h (T' - T) \frac{g}{T} \sin \theta, \quad (\text{A2})$$

where h is the parcel height, T' and T are the temperature of the soil surface and the air parcel, respectively, and θ is the slope.

The sensible heat exchange may be written (Arya, 1988):

$$\rho C_p C_H u (T' - T) = H, \quad (\text{A3})$$

where C_H is the bulk heat transfer coefficient.

From the mechanical equilibrium, we deduce that:

$$\rho C_M u^2 = \rho h (T' - T) \frac{g}{T} \sin \theta, \quad (\text{A4})$$

which, combined with (A3), gives:

$$\rho C_M u^2 = \rho h \left(\frac{H}{\rho C_p C_H u} \right) \frac{g}{T} \sin \theta, \quad (\text{A5})$$

from which we deduce that:

$$u = \left(h \left(\frac{H}{\rho C_p} \right) \frac{g}{T} \sin \theta \right)^{1/3} \left(\frac{1}{C_M C_H} \right)^{1/3}. \quad (\text{A6})$$

In practice, (A6) could not be used directly because, (i) the drag and bulk heat transfer coefficient are not measured at the sites, (ii) the measurement of H is affected by important uncertainties in nocturnal conditions, and (iii) the height of the boundary layer is not always well known. However, by supposing that the net radiation can serve as an indicator for sensible heat and by neglecting possible variations of C_M , C_H and h among sites it is possible to establish an index, for $h = 10$ m, as

$$u_{\text{adv}} = \left(10 \left(\frac{-R_{\text{net}}}{\rho C_p} \right) \frac{g}{T} \sin \theta \right)^{1/3} \quad (\text{A7})$$

that takes both the site topography and the radiative cooling intensity into account.

Appendix II

The two-dimensional continuity and tracer conservation equations are:

$$\frac{\partial u}{\partial x} + \frac{\partial w}{\partial z} = 0, \quad (\text{B1 a})$$

and

$$\frac{1}{V_m} \left(\frac{\partial uc}{\partial x} + \frac{\partial wc}{\partial z} \right) = F_s \quad (\text{B1 b})$$

where u and w represent the average velocity component in the horizontal (x) and vertical (z) directions respectively, V_m is the air molar volume and F_s represents a source term.

After integration along the vertical, they become:

$$\int_0^h \frac{\partial u}{\partial x} dz + \int_0^h \frac{\partial w}{\partial z} dz = 0, \quad (\text{B2 a})$$

and

$$\frac{1}{V_m} \left(\int_0^h \frac{\partial uc}{\partial x} dz + \int_0^h \frac{\partial wc}{\partial z} dz \right) = F_s. \quad (\text{B2 b})$$

As the vertical velocity is zero at the soil level, the integration of the last terms on the left-hand sides in Equation (B2) gives:

$$\int_0^h \frac{\partial u}{\partial x} dz + w_h = 0, \quad (\text{B3 a})$$

and

$$\frac{1}{V_m} \left(\int_0^h \frac{\partial uc}{\partial x} dz + w_h c_h \right) = F_s, \quad (\text{B3 b})$$

where w_h and c_h are, respectively, the vertical velocity and the tracer concentration at the top of the layer.

By postulating commutativity of spatial derivative and integral operations, and introducing the tracer concentration difference between level z and the top of the layer, i.e.: $\delta(z) = c(z) - c_h$, (B3) can be rewritten:

$$\frac{\partial}{\partial x} \int_0^h u dz + w_h = 0 \quad (\text{B4 a})$$

and

$$\frac{1}{V_m} \left(\frac{\partial}{\partial x} \int_0^h u \delta dz + \frac{\partial}{\partial x} \int_0^h u c_h dz + w_h c_h \right) = F_s. \quad (\text{B4 b})$$

According to (B4a), the sum of the last two terms of (B4b) is zero.

Similarity, the vertical profiles of horizontal velocity and concentration difference may be expressed as:

$$u_z = u_r f_u(z) \quad \text{and} \quad \delta_z = \delta_r f_c(z), \quad (\text{B5})$$

where, u_r and δ_r are the horizontal velocity and the tracer concentration difference measured at one given reference height, and f_u and f_c are vertical profile functions. The vertical integrals of the profile functions are therefore:

$$I_1 = \int_0^h f_u(z) dz, \quad I_2 = \int_0^h f_u(z) f_c(z) dz \quad \text{and} \quad I_3 = \int_0^h f_c(z) dz, \quad (\text{B6})$$

and Equations (B4) become:

$$I_1 \frac{du_r}{dx} = -w_h, \quad (\text{B7 a})$$

and

$$\frac{I_2}{V_m} \frac{d(\delta_r u_r)}{dx} = F_s. \quad (\text{B7 b})$$

By fixing constant vertical velocity and tracer source intensity, (B7) may be solved analytically, giving

$$u_r = u_{r0} - \frac{w_h}{I_1} x, \quad (\text{B8 a})$$

and

$$u_r \delta_r = u_{r0} \delta_{r0} + \frac{V_m F_s}{I_2} x, \quad (\text{B8 b})$$

from which the evolution with x of the tracer concentration difference is deduced:

$$\delta_r = \frac{u_{r0} \delta_{r0} + \frac{V_m F_s}{I_2} x}{u_{r0} - \frac{w_h}{I_1} x}. \quad (\text{B9})$$

(B9) shows that the tracer concentration difference tends asymptotically towards an equilibrium value given by $\delta_{\text{req}} = -\left(\frac{I_1}{I_2}\right) \frac{V_m F_s}{w_h}$. This suggests, in particular, that above homogeneous terrain and at sufficient distances from the edge the vertical concentration difference depends only on the source intensity and on the wind velocity pattern, and the horizontal gradient is zero.

References

- Arya, P.: 1988, *Introduction to Micrometeorology*. Academic Press, New York, 307 pp.
 Aubinet, M., Grelle, A., Ibrom, A., Rannik, Ü., Moncrieff, J., Foken, T., Kowalski, A.S., Martin, P. H., Berbigier, P., Bernhofer, Ch., Clement, R., Elbers, J., Granier, A., Grünwald, T., Morgenstern, K., Pilegaard, K., Rebmann, C., Snijders, W., Valentini, R., and Vesala, T.: 2000, 'Estimates of the Annual Net Carbon and Water Exchange of Forests: The EUROFLUX Methodology', *Adv. Ecol. Res.* **30**, 113–175.

- Aubinet, M., Chermanne, B., Vandenhaute, M., Longdoz, B., Yernaux, M., and Laitat, E.: 2001, 'Long Term Carbon Dioxide Exchange Above a Mixed Forest in the Belgian Ardennes', *Agr. Forest Meteorol.* **108**, 293–315.
- Aubinet, M., Heinesch, B., and Longdoz, B.: 2002, 'Estimation of the Carbon Sequestration by a Heterogeneous Forest: Night Flux Corrections, Heterogeneity of the Site and Inter-Annual Variability', *Glob. Change Biol.* **8**, 1053–1072.
- Aubinet, M., Heinesch, B., and Yernaux, M.: 2003, 'Horizontal and Vertical CO₂ Advection in a Sloping Forest', *Boundary-Layer Meteorol.* **108**, 397–417.
- Baldocchi, D., Vogel, C., and Hall, B.: 1997, 'Seasonal Variation of Carbon Dioxide Exchange Rates above and Below a Boreal Jack Pine Forest', *Agr. Forest Meteorol.* **83**, 147–170.
- Baldocchi, D., J. Finnigan, Wilson, K., Paw U. K. T., and Falge, E.: 2000, 'On Measuring Net Ecosystem Carbon Exchange Over Tall Vegetation on Complex Terrain', *Boundary-Layer Meteorol.* **96**, 257–291.
- Baldocchi, D.: 2003, 'Assessing the Eddy Covariance Technique for Evaluating Carbon Dioxide Exchange Rates of Ecosystems: Past, Present and Future', *Glob. Change Biol.* **9**, 479–492.
- Berbigier, P., Bonnefond, J. M., and Mellmann, P.: 2001, 'CO₂ and Water Vapour Fluxes for 2 Years above Euroflux Forest Site', *Agr. Forest Meteorol.* **108**, 183–197.
- Cescatti, A. and Marcolla, B.: 2004, 'Drag Coefficient and Turbulence Intensity in Conifer Canopies', *Agr. Forest Meteorol.* **121**, 197–206.
- Falge, E., Baldocchi, D., Olson, R., Anthoni, P., Aubinet, M., Bernhofer, C., Burba, G., Ceulemans, R., Clement, R., Dolman, H., Granier, A., Gross, P., Grünwald, T., Hollinger, D., Jensen, N.-O., Katul, G., Keronen, P., Kowalski, A., Ta Lai, C., Law, B., Meyers, T., Moncrieff, J., Moors, E. J., Munger, J. W., Pilegaard, K., Rannik, Ü., Rebmann, C., Suyker, A., Tenhunen, J., Tu, K., and Verma, S., Vesala, T., Wilson, K., Wofsy, S.: 2001, 'Gap Filling Strategies for Defensible Annual Sums of Net Ecosystem Exchange', *Agr. Forest Meteorol.* **107**, 43–69.
- Fan, S. M., Goulden, M. L., Munger, J. W., Daube, B. C., Bakwin, P. S., Wofsy, S. C., Amthor, J. S., Fitzjarrald, D. R., Moore, K. E., and Moore, T. R.: 1995, 'Environmental Controls on the Photosynthesis and Respiration of a Boreal Lichen Woodland: A Growing Season of Whole-Ecosystem Exchange Measurements by Eddy Correlation', *Oecologia* **102**: 443–452.
- Feigenwinter, C., Bernhofer, C., and Vogt, R.: 2004, 'The Influence of Advection on Short Term CO₂ Budget in and Above a Forest Canopy', *Boundary-Layer Meteorol.* **113**, 201–224.
- Finnigan, J.: 1999, 'A Comment on the Paper by Lee (1998): On Micrometeorological Observations of Surface-Air Exchange Over Tall Vegetation', *Agr. Forest Meteorol.* **97**, 55–64.
- Finnigan, J., Clement, R., Mahli, Y., Leuning, R., and Cleugh, H.: 2003, 'A Reevaluation of Long Term Flux Measurement Techniques. Part I: Averaging and Coordinate Totation', *Boundary-Layer Meteorol.* **107**, 1–48.
- Goulden, M. L., Munger, J. W., Fan, S.-M., Daube, B. C., and Wofsy, S. C.: 1996, 'Measurements of Carbon Sequestration by Long-term Eddy Covariance: Methods and a Critical Evaluation of Accuracy', *Glob. Change Biol.* **2**, 169–182.
- Granier, A., Biron, P., and Lemoine, D.: 2000a, 'Water Balance, Transpiration and Canopy Conductance in Two Beech Stands', *Agr. Forest Meteorol.*, **100**, 291–308.
- Granier, A., Ceschia, E., Damesin, C., Dufrêne, E., Epron, D., Gross, P., Lebaude, S., Le Dantec, V., Le Goff, N., Lemoine, D., Lucot, E., Ottorini, J. M., Pontailler, J. Y., and Saugier, B.: 2000b, 'The Carbon Balance of a Young Beech Forest', *Funct. Ecol.* **14**, 312–325.

- Grünwald, T.: 2002, *Langfristige Beobachtungen von Kohlendioxidflüssen mittels Eddy-Kovarianz-Technik über einem Altfichtenbestand im Tharandter Wald*. PhD. Dissertation, Dresden University of Technology, Dresden, Germany, 141 pp.
- Gu, L. H., Falge, E. M., Boden, T., Baldocchi, D. D., Black, T. A., Saleska, S. R., Suni, T., Verma, S. B., Vesala, T., Wofsy, S. C., and Xu, L.: 2004, 'Objective Threshold Determination for Nighttime Eddy Flux Filtering', *Agr. Forest Meteorol.*, in press.
- Havránková, K. and Sedlak, P.: 2004, 'Wind Velocity Analysis for Mountainous Site Bily Kriz', *Ekologia (Bratislava)* **23**, 46–54.
- Jacobs, A. F. G., Van Boxel, J. H., and El Kilani, R. M. M.: 1994, 'Nighttime Free Convection Characteristics within a Plant Canopy', *Boundary-Layer Meteorol.* **71**, 375–391.
- Kondo, J. and Sato, T.: 1988, 'A Simple Model of Drainage Flow on a Slope', *Boundary-Layer Meteorol.* **43**, 103–122.
- Laitat, E., Chermanne, B., and Portier, B.: 1999, 'Biomass, Carbon and Nitrogen Allocation in Open Top Chambers Under Ambient and Elevated CO₂ and in a Mixed Forest Stand. A Tentative Approach for Scaling up from the Experiments of Vielsalm', in R. J. M. Ceulemans, F. Veroustraete, V. Gond and J. B. H. F. Van Rensbergen (eds.), *Forest Ecosystem Modelling, Upscaling and Remote Sensing*, Academic Publishing, The Hague, The Netherlands, pp. 33–60.
- Lee, X.: 1998, 'On Micrometeorological Observations of Surface-air Exchange over Tall Vegetation', *Agr. Forest Meteorol.* **91**, 39–49.
- Lloyd, J. and Taylor J. A.: 1994, 'On the Temperature Dependence of Soil Respiration', *Funct. Ecol.*, **8**, 315–323.
- Manins, P. C. and Sawford B. L.: 1979, 'A Model of Katabatic Winds', *J. Atmos. Sci.* **36**, 619–630.
- Marcolla, B., Cescatti, A., Montagnani, L., Manca, G., Kerschbaumer, Minerbi, S.: 2005. 'Role of advective fluxes in the carbon balance of an alpine coniferous forest' *Agr., Forest Meteorol.* (in press).
- Moncrieff, J. B., Malhi, Y., and Leuning, R.: 1996, 'The Propagation of Errors in Long-Term Measurements of Land-Atmosphere Fluxes of Carbon and Water', *Glob. Change Biol.* **2** 231–240.
- Montagnani, L.: 1999, *Flussi di carbonio in un ecosistema alpino*. PhD Dissertation, University of Padova, 134 pp.
- Papale, D. and Valentini, R.: 2003, 'A New Assessment of European Forests Carbon Exchanges by Eddy Fluxes and Artificial Neural Network Spatialization', *Glob. Change Biol.* **9**, 525–535.
- Paw, U. K. T., Baldocchi, D. D., Meyers, T. P., and Wilson, K. B.: 2000, 'Correction of Eddy-Covariance Measurements Incorporating both Advective Effects and Density Fluxes', *Boundary-Layer Meteorol.* **97**, 487–511.
- Perrin, D., Laitat, E., Yernaux, M., and Aubinet, M.: 2004, 'Modélisation de la réponse des flux de respiration d'un sol forestier selon les principales variables climatiques', *Biotechnol. Agron. Soc. Env.* **8**, 15–25.
- Pumpainen, J., Ilvesniemi, H., Perämäki, M., and Hari, P.: 2003, 'Seasonal Patterns of Soil CO₂ Efflux and Soil Air CO₂ Concentration in a Scots Pine Forest: Comparison of Two Chamber Techniques', *Glob. Change Biol.* **9**, 371–382.
- Schimel, D. S.: 1995, 'Terrestrial Ecosystems and the Carbon Cycle', *Glob. Change Biol.* **1**, 77–91.
- Staebler, R. M. and Fitzjarrald, D. R.: 2004, 'Observing Subcanopy CO₂ Advection', *Agr. Forest Meteorol.* **122**, 139–156.
- Swinbank, W. C.: 1951, 'The Measurement of Vertical transfer of Heat and Water Vapour by Eddies in the Lower Atmosphere', *J. Meteorol.* **8**, 135–145.

- Tennekes, H. and Lumley, J. L.: 1972, *A First Course in Turbulence*. MIT Press. Cambridge, Mass, 399 pp.
- Valentini, R. (ed.): 2003. *Fluxes of Carbon, Water and Energy of European Forests*. Ecological Studies 163, Springer-Verlag, Berlin, 274 pp.
- Watson, R. T., Noble, I. R., Bolin, B., Ravindranath, N. H., Verardo, D. J., and Dokken, D.J. (eds.), 2000. *Land Use, Land-Use Change, and Forestry. Special Report of the Intergovernmental Panel on Climate Change*. Cambridge University Press, U.K. 375 pp.
- Wilczak, J., Oncley, S. P., and Stage, S. A.: 2001, 'Sonic Anemometer Tilt Correction Algorithms.' *Boundary-Layer Meteorol.* **99**, 127–150.